Supporting Information for

Robust Adaptive Pathways for Long-Term Flood Control in Delta Cities: Addressing Pluvial Flood Risks under Future Deep Uncertainty

Contents of this file

Text 1 Data and scenarios

First, we built a comprehensive database using multi-source data, including basic geographic information, meteorological and hydrological data, and urban flood control data. The data utilized in this study comprise rainfall data, drainage capacity data, elevation data, socioeconomic statistics, and land use data (Table S1).

1）Rainfall data. The hourly rainfall data of 11 meteorological stations in Shanghai, including Xujiahui (representing the central urban area), Minhang, Baoshan, Pudong, Jiading, Nanhui (now part of Pudong New Area), Jinshan, Qingpu, Songjiang, Fengxian and Chongming, were taken from 16:00 to 19:00 on September 13, 2013. The station observation data are spatially interpolated to the 30m resolution grid as the precipitation input data of the model. The diachronic precipitation data of 11 stations in the central urban area and counties of Shanghai center were collected to study the temporal variation trend and spatial distribution characteristics of each diachronic extreme precipitation. In addition, this study also collected the "110" citizen alarm records during the "913" period as the model simulation verification data, which includes the location of alarm points and the submergence depth of alarm points.

2) Drainage Capacity Data. Due to the lack of detailed pipeline data, this study utilizes generalized 2013 Shanghai drainage capacity data to represent the design standards of each drainage unit. The central urban area within Shanghai's outer ring road is divided into 284 drainage units, categorized by drainage capacity into three levels. Units with poor drainage capacity are typically older combined rainwater-sewage pipe networks in the main urban area, designed for a standard of 27 mm/h. Newer drainage units are generally built to meet a one-year rainstorm standard, with a capacity of 36 mm/h. Additionally, the Expo site features a higher drainage standard of 50 mm/h (He et al., 2017).

3) Elevation data. The digital elevation model (DEM) used in this study has a 30-meter resolution and is derived from detailed observations by NASA's Terra satellite. The raw DEM data were processed to fill depressions and eliminate false depressions. Land use data were then used to extract residential and commercial areas, and elevation was corrected by 15 mm for these zones.

4) Socioeconomic Statistics. The socioeconomic data used in this study were primarily sourced from the *Shanghai Statistical Yearbook*, published annually by the Shanghai Municipal Bureau of Statistics. Key entries include district and county population, GDP, public green area, average household properties, and average construction costs.

5) Land use data. Land use data were derived from the 2015 remote sensing monitoring dataset of China's land use status, released by the Institute of Geographical Sciences and Natural Resources Research, Chinese Academy of Sciences. For this study, 30-meter resolution land use data for Shanghai were selected, encompassing nine categories and 32 land use types. These categories were reclassified into 10 land use types, including industrial and commercial land, new-style residential areas, and natural villages.

Table S1 Data information description

Type of data	Data resolution	Data description
Rainfall information	30m	Hourly rainfall data from 11 weather stations
Drainage capacity		284 drainage units with design standards of 27mm/h, 36mm/h and 50mm/h respectively.
Elevation	30m	Advanced Spaceborne Thermal Emission and Anti-Radiometer GDEM Data with ASTER Sensors
Socioeconomic Statistics		District and sub-district population, district and county GDP, area and investment of public green space, average indoor property and average construction cost
land use	30m	Industrial land, commercial land, new housing

Scenarios generation

Three uncertainty factors—future rainfall (α), the urban rain island effect (β), and the decrease in drainage capacity (γ)—were selected to generate future extreme rainstorm scenarios (Table S2). The range for future rainfall (α), between 7% and 18%, was derived from a daily downscaled dataset of 21 GCM simulations from CMIP5, under both

RCP4.5 and RCP8.5 emission scenarios, for the Yangtze River Delta region. This dataset includes nine grid cells covering Shanghai city by 2050 (Wang et al., 2015).

For the urban rain island effect (β), previous research (Liang and Ding, 2017) found that the total precipitation during heavy rainfall events increased at central urban sites (Pudong and Xujiahui) and nearby suburban sites (Minhang and Jiading) by rates of 21.7–25 mm/10 years. By the 2050s, this effect is projected to result in an approximate margin of increase (β_1) between 10% and 20% for central urban areas (Xujiahui and Pudong) during heavy rainfall events, while suburban sites could experience a slight decrease (β_2) ranging from −0.076% to −0.038%.

To account for uncertainties in sea-level rise, land subsidence, and other factors contributing to drainage system degradation, the reduction in existing drainage system capacity (γ) is assumed to range between 0% and 50% (Hu et al., 2019). Based on these ranges for the three uncertainty factors, 100 future scenarios were generated using Latin Hypercube Sampling (LHS).

Table S2. Future uncertain factors and range of uncertainties in 2050

Uncertain factors	Range of uncertainties
Future rainfall (α)	(α)increase from 7% to 18%
Urban rain island effect (β)	(β)increase from 10% to 20% in central region (Xujiahui and Pudong rain gauges), decrease from -0.076% to -0.038% (other 9 rain gauges in Shanghai)
Decrease of drainage capacity (γ)	(γ) decrease from 0 to 50% due to the anthropogenic land subsidence and sea level rise

Text 2 Pluvial flood risk and solution performance

The hydrological model SCS-CN (Soil Conservation Service Curve Number) is characterized by simple parameters and easily accessible data, making it widely applicable in Shanghai. To address challenges related to multi-scenario, multi-model, and large-scale simulation calculations, Hu et al. (2023) developed the Shanghai Urban Inundation Model (SUIM) based on SCS-CN. The SUIM aims to provide a rapid and integrated model for minimizing flood risk and offers technical support for evaluating the effectiveness of adaptation options in mitigating urban pluvial flood risks.

The SUIM integrates sub-modules for rainfall simulation, hydrology, spatial statistics, risk assessment, and option evaluation to enable comprehensive risk assessment

and adaptation option evaluation. These coupled sub-modules optimize the simulation process and enhance computational efficiency. The model utilizes a PostgreSQL database, supporting GIS spatial data storage and analysis, including operations such as feature clipping, layer extraction, coordinate transformation, and spatial interpolation. With its regular grid structure, the model ensures fast calculations, logical simplicity, and automated processing capabilities.

The integrated SUIM model is suitable for various applications, including historical event backtracking, inundation forecasting and early warning, future scenario evaluation, and hydraulic engineering pre-planning. The overall architecture and process flow are illustrated in Figure S1.

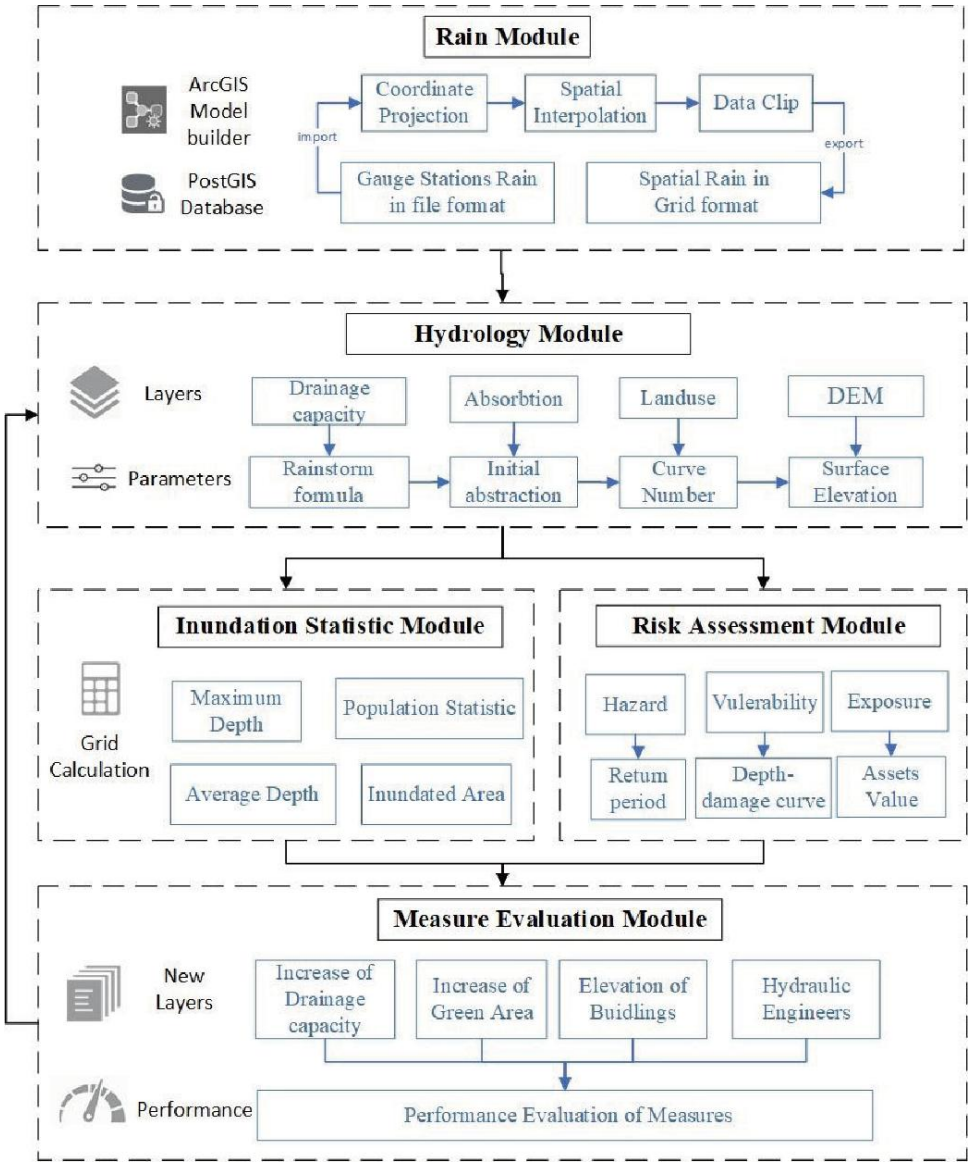

Figure S1 Structure of Shanghai urban inundation model

In order to compare and quantitatively evaluate the performance of adaptation options, this study constructs different adaptation options and their combinations, simulates the differences in the depth of waterlogging and the affected population before and after the implementation of the adaptation options, and evaluates and quantifies the performance under different climate scenarios in the future. In addition to the baseline scenario, the future 100 scenarios for each adaptation option and its combination are simulated (Figure S2). The specific parameters of the simulation setting up and the performance results are seen as Table S3, S4.

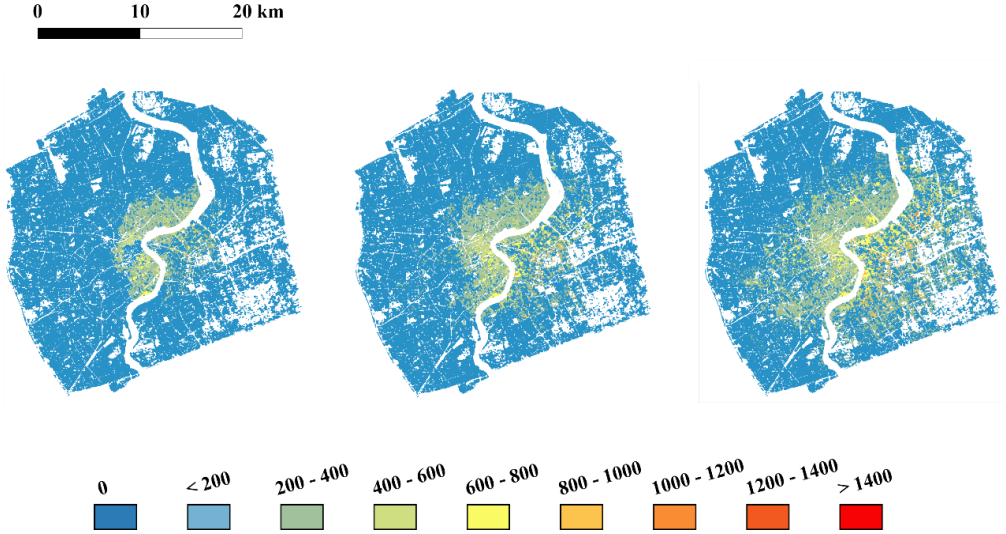

Figure S2. Comparison of damage/loss (thousand RMB/900m^2 grid): Sc-53 (left), Sc-3 (middle), Sc-11 (right)

Table S3 Simulation setting-up to the performance of adaptation options

Experiment	Option	Experimental program	Performance	Abbreviation
0	baseline	Model effect verification	/	
1	baseline	City Defense Capability Simulation	/	
2	Drainage	Increase drainage capacity to 1/5-year	low	Dr
3	Green area	Increase surface water permeability	low	GA
4	deep tunnel 1	absorb 30% of rainfall	middle	Tun30
5	deep tunnel 2	absorb 50% of rainfall	middle	Tun50
6	deep tunnel 3	absorb 70% of rainfall	high	Tun70
7	Combination 1	Green area + Drainage	middle	D+G
8	Combination 2	Green area + Deep tunnel 1	middle	G+Tun30
9	Combination 3	Green area + Deep tunnel 2	high	G+Tun50
10	Combination 4	Green area + Deep tunnel 3	overflow	G+Tun70
11	Combination 5	Drainage + Deep tunnel 1	middle	D+Tun30

12	Combination 6	Drainage + Deep tunnel 2	high	D+Tun50
13	Combination 7	Drainage + Deep tunnel 3	overflow	D+Tun70
14	Combination 8	Green area + Drainage + Deep tunnel 1	high	D+G+Tun30
15	Combination 9	Green area + Drainage + Deep tunnel 2	overflow	D+G+Tun50
16	Combination 10	Green area + Drainage + Deep tunnel 3	overflow	D+G+Tun70
	…	…	…	…

Table S4 Statistic information of options combinations

	Min	25%	Mid	75%	Max	Std	Mean	Range
Dr	0.08	0.11	0.16	0.37	0.80	0.20	0.25	0.72
GA	0.09	0.11	0.17	0.38	0.73	0.18	0.26	0.64
Tun30	0.17	0.20	0.32	0.54	0.89	0.21	0.39	0.72
D+G	0.18	0.37	0.70	0.89	0.94	0.27	0.62	0.76
Tun50	0.33	0.65	0.85	0.91	0.99	0.21	0.74	0.66
D+G+T30	0.61	0.80	0.89	0.91	0.99	0.08	0.85	0.38
Tun70	0.79	0.81	0.89	0.91	0.99	0.05	0.87	0.2

Text 3 Risk assessment

The assessment of asset value encompasses commercial assets, including commercial and residential buildings, as well as household property. Exposure analysis is conducted by overlaying flood scenarios with asset values across multiple scenarios. The calculation formula is as follows:

$$B_{\exp osure} = A_{asset} \cap H \quad (1)$$

where $B_{exposure}$ is the exposed assets; A_{asset} is the value of land use assets; and H is hazard.

A comprehensive evaluation of asset exposure was conducted, including indoor property, business, and building losses, using a depth-damage curve. Based on the findings of previous studies (Ke, 2014), this study developed an inundation depth-vulnerability curve tailored to the study area, as detailed in Table S5.

Table S5 Depth-damage curve of inundation depth in Shanghai

Category	Inundation depth (m)						
	<0.5	0.5-1.0	1.0-1.5	1.5-2.0	2.0-2.5	2.5-3.0	>3.0
Public	3%	7%	12%	14%	18%	20%	25%

building							
Commercial Building	5%	9%	13%	18%	22%	27%	31%
Industrial building	3%	8%	11%	15%	19%	2%	25%
Residential building	3%	65	9%	12%	16%	19%	22%
Household property	9%	19%	26%	33%	38%	46%	58%

The damage loss of pluvial flood is calculated in SUIM by each inundation of the scenarios. The statistic information is then calculated at grid level.

$$T_{loss} = \sum_{i=1,j=1}^{n} (V_i \times R_j) \quad (2)$$

where T_{loss} is the total loss in the study region; V_i is the *i-th* exposed asset value of the elements at risk; R_j is the *j-th* loss rate of the elements at risk in different water depth intervals.

To evaluate flood control options, pluvial flood statistics are quantified through re-simulations under the baseline scenario in SUIM. For example, the effectiveness of drainage capacity enhancements is assessed by calculating the loss reduction rate compared to baseline options under future scenarios.

$$RRR = \frac{T_{loss}{}' - T_{loss}}{T_{loss}} \times 100\% \quad (3)$$

where $T_{loss}{}'$ is the flood damage after implementing a flood control option; accordingly, *Performance* calculates the reduction rate of loss against its baseline scenario.

Text 4 Benefit-cost analysis

Benefit and cost are indispensable considerations when making investment decisions. Generally, the cost of a option is proportional to its benefit in terms of flood risk reduction. Engineered solutions with superior performance often incur higher costs and require longer construction periods. This study evaluates the economic viability of various adaptation options by calculating their benefit-cost ratios.

For cost assessment, the life cycle cost analysis (LCCA) method is employed. This method considers the initial construction cost of options, the average annual operation

and maintenance costs, the residual value of the facility at the end of its service period, and its effective lifespan. The costs of options determined using LCCA are detailed in Table S6 of the Supplementary Material. Internationally, the net present value of benefits (PVB) and costs (PVC) are used to represent benefits and expenses, respectively (Liao et al., 2014). The formula for calculating cost-benefit ratios is as follows:

$$\frac{B}{C} = \frac{PVB}{PVC} \tag{3}$$

Given that the objective of this study is not to calculate the direct risk of extreme waterlogging in the future, and the absolute value of the risk is too large to allow for meaningful comparisons, the net present value of the benefit (PVB) is selected as the inundation risk reduction rate (RRR) before and after the implementation of the options, rather than the waterlogging risk reduction value. The life cycle cost analysis formula is as follows:

$$PVC_Y = IC_Y + \sum_{t-0}^{T} fr_t MO_t - fr_T SV_t \tag{4}$$

The costing of options includes initial cost (*IC*), annual maintenance and operations (*MO*) and residual value (*SV*); fr_t is the present value factor for the discount rate *r* in a particular year *t*; the present value factor for the discount rate r at the end of n years in the design life of fr_T. The life cycle is designed to be 20-50 years. and the investment horizon is *T* years. Taking into account the economic growth rate, the study assumes a discount rate of 5% in Shanghai (Ke, 2015).

We used life cycle cost analysis estimates the cost of adaptation options, includes the drainage (Dr), public green area (GA), the 30% absorption capacity of the deep tunnel (Tun30), the 50% absorption capacity of the deep tunnel (Tun50), and the 70% absorption capacity of the deep tunnel (Tun70). Table S6 presents that the LCCA the order from low to high is Dr < Tun30 < GA < Tun50 < Tun70; among them, Dr has the lowest drainage enhancement, while Tun70 has the highest total cost of 70% absorption capacity of underground deep tunnels.

From the perspective of annual average cost (AAC), the order of cost from low to high is GA <Dr < Tun30 <Tun50<Tun70. The average annual cost of low impact solutions for “public green area” is the lowest, and the average annual cost of “grey”

options is high. On the basis of the above five basic options, two additional options, (D + G) “drainage enhancement + public green area increase” and (D + G + Tun30) “drainage enhancement + public green area increase + 30% absorption capacity of deep tunnels” are added, and calculate the average annual cost and total cost respectively.

The results in Table S6 show that the average annual cost (39-41 million USD/ year) of drainage enhancement (Dr), public green area increase (GA) and 30% absorption capacity of underground deep tunnel (Tun30) is close to the total cost (1918-2570 million USD). However, the average disaster loss reduction rate is low, less than 0.39, and the performance is unsatisfactory in the face of extreme flooding scenarios. In terms of risk reduction rate, the risk reduction rate (0.62) of the combined option of drainage enhancement and public green area (D+G) is greater than the risk reduction rate of a single option (0.51), indicating that the benefit of the combined options are better than that of the single option. Although the average annual cost and total cost of the deep tunnel with 50% absorption capacity (Tun50) and 70% absorption capacity (Tun70) are relatively high, second only to drainage enhancement + public green area (D+ G) and drainage enhancement + public green area + 30% absorption capacity of deep tunnel (D+G+Tun30), the average disaster loss reduction rate is also relatively high.

Table S6 Life cycle cost estimates for five adaptation options

Option	Unit cost (million/km, million/km^2)	Unit (km,km^2)	Maintenance costs	Life span	Total cost （million)	Residual value （million)	Average annual cost （million)
Dr	14	118	2%	50	1,918	52	39
GA	86	30	2%	70	2,570	36	37
Tun30	43	22	5%	50	2,010	29	41
Tun50	43	37	5%	50	3,350	49	68
Tun70	43	52	5%	50	4,690	68	95

*Note: Considering that public green space generally does not have a useful life period, the period is set to 70 years. The cost of Dr and GA is referred to Xie et al., 2017

Text 5 Metrics value of multi-objective trade-off analysis

All the metrics’ value of the options and their combinations are normalized from 0 to 1, and then equally weighted to sum score as seen in Table S7. The results shows that Tun50 achieves the best cost-benefit ratio, and Tun 70 has the highest ARRR and valid

period. In comparison, D+G+Tun30 has the highest flexibility and sum of metrics (3.05), showing the best performance among all options.

Table S7 Metrics' value of all options for multi-objective trade-off analysis

Option	GA	Dr	Tun30	D+G	Tun50	D+G+Tun30	Tun70
ARRR	0	0.10	0.47	0.50	1.00	0.90	0.93
Cost-benefit	0.12	0.00	0.70	0.38	1.00	0.19	0.61
Flexibility	0	0	0	0.67	0.33	1.00	0.33
Valid period	0.08	0.14	0.20	0.22	0.58	0.96	1.00
Sum score	0.22	0.26	1.38	1.77	2.91	3.05	2.87

Reference

Chen, H.-P., Sun, J.-Q., Li, H.-X. 2017. Future changes in precipitation extremes over China using the NEX-GDDP high-resolution daily downscaled dataset. Atmospheric and Oceanic Science Letters, 10(6), 403-410. DOI: 10.1080/16742834.2017.1367625.

Chen, Y., Samuelson, H.W., Tong, Z. 2016. Integrated design workflow and a new tool for urban rainwater management. J. Env. Manag. 180, 45-51.

Chung, W. H., Wang, I.T., Wang, R.Y. 2010. Theory-based SCS-CN method and its applications. J Hydrol Eng 15(12):1045–1058.

Green, C. H. 2010. Coastal cities: assets at risk and depth-damage curves; report prepared for the OECD, Middlesex University.

Han J C. 2014. Optimization of upgrading schemes of drainage systems by InfoWorks ICM software, 2014. China Water & Wastewater. 30 (11), 34-38.

He, B., Chen, C., Zhou, N. 2003. Urbanized area runoff coefficient and its application. Shanghai Environmental Science 22(7), 472-476. (In Chinese).

Hu, H., Tian, Z., Sun, L., et al. (2019). Synthesized trade-off analysis of flood control solutions under future deep uncertainty: An application to the central business district of Shanghai. Water Res, 166, 115067.

Hu H, Yang H, Wen J, Zhang M, Wu Y. An Integrated Model of Pluvial Flood Risk and Adaptation Option Evaluation in Shanghai City. Water. 2023; 15(3):602.

Ke, Q. 2014. Flood Risk Analysis for Metropolitan Areas – A Case Study for Shanghai. PhD Dissertation, Technology of Delft University, Department of Hydraulic Engineering.

Liang, P., Ding, Y.H., 2017. The long-term variation of extreme heavy precipitation and its link to urbanization effects in Shanghai during 1916-2014. Adv. Atmos. Sci. 34, 321- 334.

Mishra, S. K., Singh, V. P. 2003. Soil conservation service curve number (SCS-CN) methodology. Kluwer Academic Publishers, Dordrecht.

Pan X.-Z., Zhao, Q.-G., Chen J., Liang Y., Sun C. 2008. Analyzing the variation of building density using high spatial resolution satellite images: the example of Shanghai City. Sensors. 8(4):41-2550.

Quan, R., Liu, M., Hou, L., Lu, M., Zhang, J.L., Ou, D.N. 2009. Impact of land use dynamic change on surface runoff: A case study on Shanghai Pudong New District. J Catastr. 24. 44-49.

Shi, Y. 2010. Urban vulnerability assessment under the disaster scenarios: case study in Shanghai. East China Normal University. in Chinese

Wen, J. H., Huang, H., Chen, K, et al. 2012. Probabilistic Community-based Typhoon Disaster Risk Assessment: A Case of Fululi Community, Shanghai. Scientia Geographica Sinica, 32 (3): 348-355.

Xie, J., Chen, H., Liao, Z., Gu, X., Zhu, D., & Zhang, J. (2017). An integrated assessment of urban flooding mitigation strategies for robust decision making. Environmental Modelling & Software, 95, 143-155. doi:10.1016/j.envsoft.2017.06.027

Yin, Z. E., Xu, S. Y., Yin, J., et al. 2010. Small-scale Based Scenario Modeling and Disaster Risk Assessment of Urban Rainstorm Water-logging. Acta Geographica Sinica 65(5): 553-561.

Wang, X., Yin, Z.-E., Chi, X.-X., Yin, J., 2015. Characteristics of different magnitude precipitation change in Shanghai during 1961d2010. J. Earth Env. 6 (3), 161-167 (In Chinese).

Wang, J., Yi, S., Li, M., Wang, L., Song, C., 2018. Effects of sea level rise, land subsidence, bathymetric change and typhoon tracks on storm flooding in the coastal areas of Shanghai. Sci. Total Environ. 621, 228-234.

Wu, W., Liang, Z., Liu, X. 2018. Projection of the daily precipitation using CDF-T method at meteorological observation site scale. Plateau Meteorology (in Chinese), 37(3), 796-805. (In Chinese).